Zeitschrift: Eclogae Geologicae Helvetiae
Herausgeber: Schweizerische Geologische Gesellschaft
Band: 86 (1993)
Heft: 2

Artikel: Oblique slip and block rotation along the Engadine line
Autor: Schmid, Stefan M. / Froitzheim, Nikolaus
DOI: https://doi.org/10.5169/seals-167253

Eclogae geol. Helv. 86/2: 569–593 (1993)

0012-9402/93/020569-25 $ 1.50 + 0.20/0
Birkhäuser Verlag, Basel

Oblique slip and block rotation along the Engadine line

By STEFAN M. SCHMID and NIKOLAUS FROITZHEIM [1])

ABSTRACT

The vectors of movement along the Engadine line rapidly change along strike. Paleostress analysis using minor faults related to the master fault predicts E–W extension and a sinistral horizontal component of movement all along a single Engadine line, well defined between Maloja and Zernez. Downfaulting of the SE block is predicted for the NE part, pure strike-slip for the central part, and relative uplift of the SE block for the SW part of the Engadine line. These predictions are in accordance with a rotation model based on large scale nappe correlations in the Upper Engadine and retrodeformation of movements along the Engadine line. Rotation of the SE block by 10.5° around a horizontal axis yields 2.8 km vertical and horizontal components near Maloja, 3.1 km pure horizontal movement near Samedan and 3.2 km vertical and horizontal components at S-chanf.

Block rotation and oblique slip are interpreted to result from post-collisional shortening taking place near the Oligocene-Miocene boundary. In the SW this shortening resulted in vertical extrusion of the Bergell area, while lateral extrusion toward the E predominated in the NE. The Engadine line straddles a transitional area affected by block rotations. The rotation model yields new results regarding nappe correlation across the NE part of the Engadine line. The position of the Ela nappe is Lower Austroalpine and a continuation into the Upper Austroalpine Ortler zone is rejected. The Silvretta-Languard-Sesvenna basement units originally occupied similar tectonic positions directly above the Lower Austroalpine or Penninic units. They were first dissected by normal faulting of inferred Late Cretaceous age and then displaced by the later movements along the Engadine line.

ZUSAMMENFASSUNG

Die Bewegungsvektoren an der Engadiner Linie ändern sich im Streichen rasch. Die Paläospannungsanalyse benützt mit der Hauptverwerfung im Zusammenhang stehende kleine Verwerfungen und prognostiziert E–W Extension und sinistralen Versatz an der zwischen Maloja und Zernez gut definierten Engadiner Linie. Im NE Sektor wird eine Absenkung des SE-Flügels, im zentralen Teil reine Blattverschiebung und im SW Sektor Hebung des SE-Flügels vorausgesagt. Diese Befunde stimmen mit einem Rotationsmodell überein. Dieses Modell beruht auf Deckenkorrelationen im Oberengadin und daraus resultierender Retrodeformation der Bewegungen an der Engadiner Linie. Eine Rotation des SE-Blockes um 10.5° um eine horizontale Drehachse ergibt je 2.8 km horizontale und vertikale Bewegungskomponenten bei Maloja, 3.1 km reine Blattverschiebung bei Samedan und je 3.2 km horizontale und vertikale Komponenten bei S-chanf.

Blockrotation und schräge Bewegung werden als Resultat der post-kollisionalen Einengung an der Wende Oligocän-Miocän gedeutet. Im SW führt diese Einengung zu vertikaler Extrusion des Bergell-Gebietes, währenddem weiter im NE laterale Extrusion nach E dominiert. Die Engadiner Linie fällt mit einem Übergangsgebiet zusammen, in welchem Blockrotationen auftreten. Das Rotationsmodell liefert neue Anhaltspunkte für die Dekkenkorrelation über den NE Teil der Linie. Die Stellung der Ela-Decke ist unterostalpin, eine Verbindung mit der oberostalpinen Ortlerzone wird abgelehnt. Das Grundgebirge der Silvretta-, Languard- und Sesvenna-Decken befand sich ursprünglich in einer einheitlichen tektonischen Position, direkt über dem Unterostalpin oder Penninikum. Es wurde zuerst durch vermutliche spätkretazische Abschiebungen und später durch die Bewegungen an der Engadiner Linie in einzelne Blöcke zerlegt.

[1]) Geologisch-Paläontologisches Institut, Bernoullistr. 32, CH-4056 Basel.

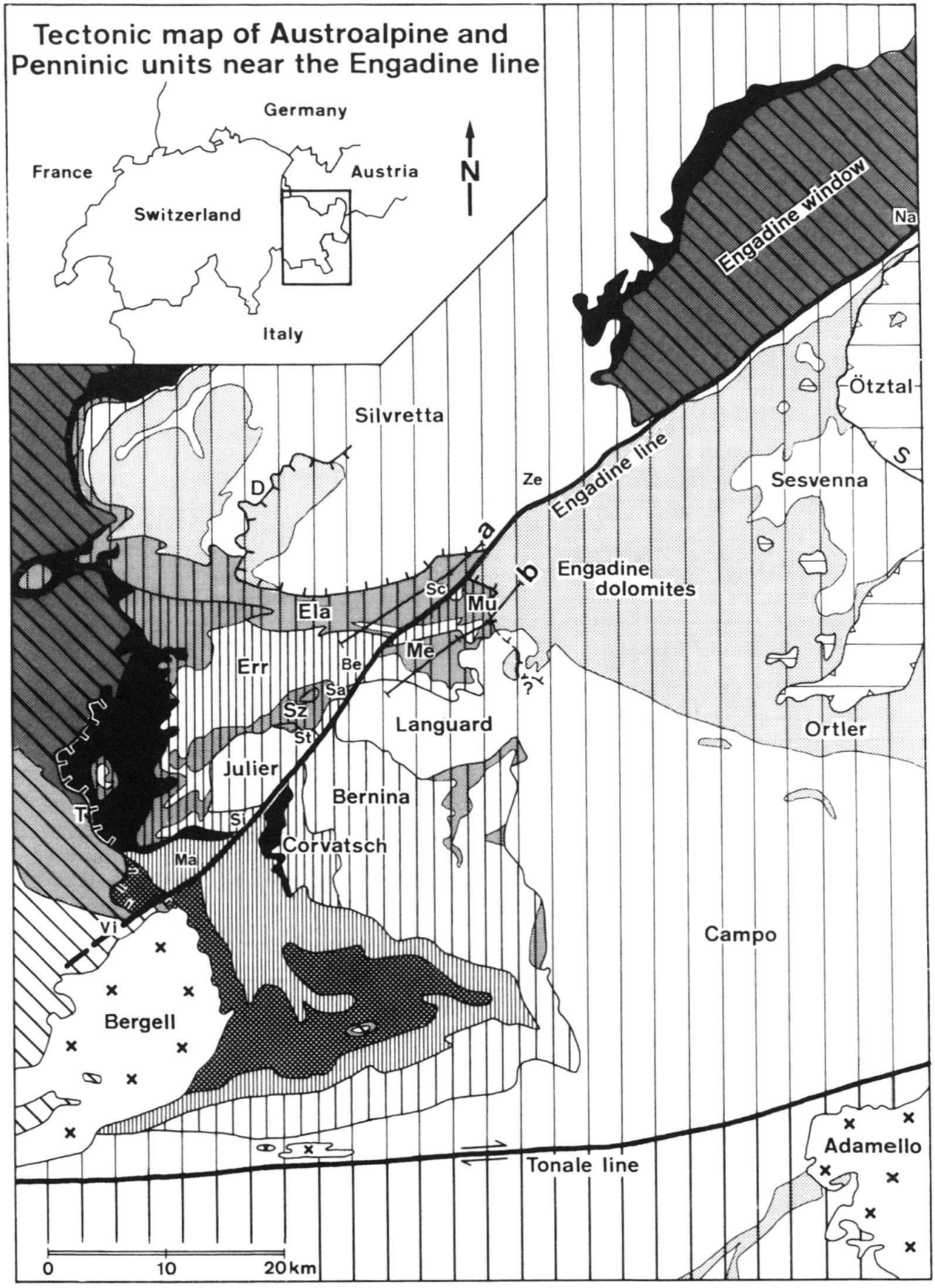

Fig. 1. Tectonic map of SE Switzerland. Profile traces refer to Fig. 7.

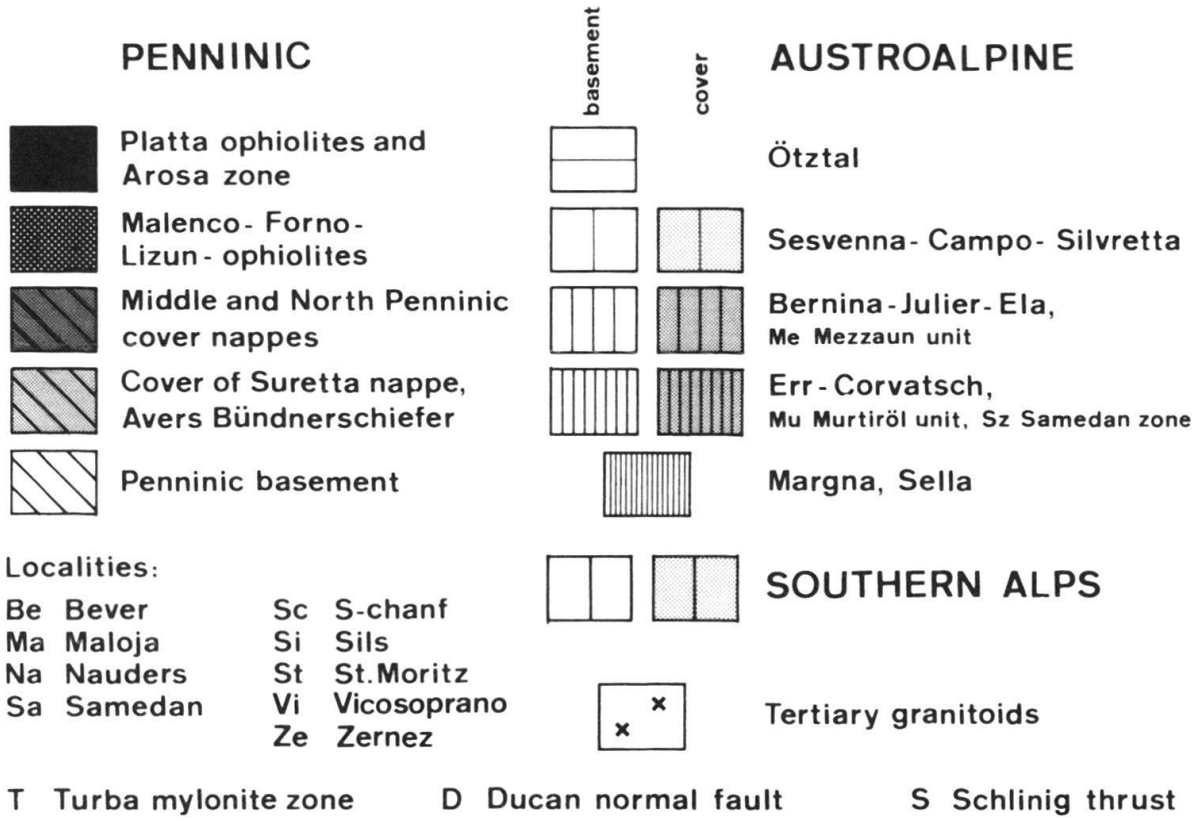

Legend to Fig. 1

1. Introduction

On the tectonic map of Switzerland (Spicher 1980) the Engadine line appears as a major SW–NE trending steeply inclined discontinuity, affecting a pre-existing nappe pile including Penninic units (Val Bregaglia and Engadine window) and, additionally, Lower and Upper Austroalpine units (Fig. 1). Val Bregaglia (Bergell) and upper Inn valley (Engadine) are the morphological expression of this fault zone. While the notion of a single fault zone referred to as Engadine line is relatively recent (Trümpy 1977) individual segments have already been noted by earlier workers, particularly in the Lower Engadine ("Nordwestliche Randlinie", e.g. Spitz & Dyhrenfurth 1914). Subsequent geologists, in particular Staub (1921, 1946) who produced excellent geological maps virtually calling for a throughgoing discontinuity, largely ignored the Engadine line in favour of adventurous nappe correlations across the alluvial cover of the valley floor (see tectonic map in Staub 1946), hiding a large portion of the fault trace. Trümpy (1977) gave the first and so far only comprehensive description of this fault zone which he interpreted as a sinistral strike-slip fault with lateral displacement varying between 3–6 km in the Upper Engadine and up to 20 km in the Lower Engadine. The latter estimate is based on correlating Silvretta and Oetztal nappes as a coherent thrust block above the Sesvenna basement and its sedimentary cover (Engadine Dolomites). This interpretation implies varying amounts of offset parallel to the Engadine line and hence the transformation of large amounts of strike-slip displacement in the Lower Engadine into synchronous thrusting within the country rocks (base of the Oetztal nappe and/or base of the Silvretta nappe).

While vertical components of offset across the Engadine line may in fact simply be apparent, resulting from strictly horizontal strike-slip movements affecting a pile of E-dipping nappes, some evidence for "true" vertical components of movement is available, although of extremely conflicting nature. Additionally, such evidence often relies on particular concepts as to how exactly nappe units have to be correlated across the Engadine line. Hence the determination of movement vectors is not only interesting for a better understanding of this late Alpine fault as such but also for restoring the original nappe pile.

This is particularly true for the lower Engadine, where Eugster (1971, 1985), following Wenk (1934), correlated the Silvretta nappe with the basement of the Engadine Dolomites (Sesvenna basement in general and "Oberer Gneiszug" in particular). Such a correlation calls for a substantial vertical component of movement which can no longer be caused by left lateral movement of inclined nappe contacts (Fig. 1). According to Eugster (1971, 1985) the "Nordwestliche Randlinie" of the Lower Engadine has nothing to do with the Engadine line in the upper Engadine but finds its continuation SE of S-chanf and at the base of the Ortler unit. For Eugster (1971) this fault zone represents a décollement horizon between basement (Campo-Silvretta-Sesvenna) and its cover (Engadine Dolomites and Ortler zone) of unspecified nature (thrust or normal fault?). Schmid & Haas (1989), following Eugster's arguments in terms of nappe correlations, postulated the existence of a normal fault in the Lower Engadine, associated with updoming and unroofing of the Engadine window. A minimum vertical component of 4 km is inferred at the SW termination of the Engadine window (Fig. 5 and 13 in Schmid & Haas 1989). Near Nauders, the base of the Oetztal nappe (Schlinig thrust) merges with the Engadine line, suggesting a considerably increasing component of vertical movement towards the NE.

Between S-chanf and Bever, however, a half window of Lower Austroalpine units SE of the Engadine line (Murtiröl and Mezzaun area, Fig. 1), is facing the Ela nappe NW of the Engadine line. If the Ela nappe is considered as an Upper Austroalpine unit (as assumed by most authors), this suggests uplift of the SE block (half window of Lower Austroalpine units) rather than the NW block (Ela nappe), as postulated for the Lower Engadine. Trümpy (1977) interprets updoming of this half window to be due to folding directly coupled with sinistral movements along the Engadine line.

According to the generally accepted nappe correlations, the sense of apparent vertical displacement changes again near Samedan. There the Upper Austroalpine Languard nappe faces the Lower Austroalpine Err nappe on the NW side of the valley floor, indicating uplift of the NW block.

While conflicting evidence regarding vertical components of movements so far heavily depended on uncertain nappe correlations and on assumptions regarding possible transformations of the movement into deformation of the country rocks, the evidence is somewhat clearer between Sils and Maloja (Fig. 1). Nappe correlations are well established, in particular regarding the Margna nappe enveloped by two ophiolitic units (Montrasio & Trommsdorff 1983). Liniger & Guntli (1988), based on a displacement vector deduced by Mützenberg (1986), inferred a left lateral displacement (1.1 km) combined with a vertical component (2.2 km uplift of the SE block). Hence, the apparent vertical component changes once again in respect to the situation near Samedan. Wenk (1984) proposes a brittle-ductile transition along the Engadine line in the Upper Val

Bregaglia. He correlates mylonites at the northern end of and within the Gruf complex with brittle faulting along what he calls Maloja line. On the other hand, he denies a continuation of the Maloja line towards the NE and beyond Sils. This latter conclusion is based on an erroneous interpretation of internal deformation within the Margna nappe around Sils lake to be associated with movements along the Maloja line (see Liniger & Guntli 1988). A brittle-ductile transition into the Val Bregaglia area however is very plausible since no continuation of the Engadine line in terms of a brittle fault zone can be traced into the lower Val Bregaglia and across the Mera valley.

The outcrops near Maloja provide the only available time marker for dating movements along the Engadine line. Contact-metamorphosed country rocks of the Bergell granodiorite (30.1 Ma, von Blanckenburg 1992 confirming older determinations by Grünenfelder & Stern 1960) are cataclastically deformed. Hence the movements postdate intrusion and cooling of the Bergell aureole, but no upper time mark is available at the moment. The K/Ar biotite age of 27.0 Ma obtained by Giger (1991, KAW 328) for contact-metamorphosed country rocks near Maloja indicates rapid cooling, and it is feasible that movements along the Engadine line already occurred during the Late Oligocene. The expected brittle-ductile transition towards the Mera valley makes such an early age highly probable in view of the cooling history of the Novate-Codera region (Jäger et al. 1967, Purdy & Jäger 1976, Wagner et al. 1977, see discussion in Giger 1991) which indicates temperatures below 300 °C at or soon after the Oligocene-Miocene boundary. This precludes ductile deformation in that region at some later stage during the Miocene.

One of the purposes of this study is a clarification of the following questions of regional interest, immediately following from the foregoing discussion: (1) Does a single Engadine line as proposed by Trümpy (1977) and mapped out in the Tectonic map of Switzerland (Spicher 1980) exist at all or do different fault zones accidentally link up along a linear array? (2) What is the extent and nature of contemporaneous deformation of the country rocks to both sides of the line? (3) If there is a single Engadine line in the sense of Trümpy (1977), what is the movement vector along this fault zone and what are the consequences in terms of uncertain nappe correlations regarding the Austroalpine nappe pile to the NE of Sils?

Additionally, a new method for the determination of the movement vector based on paleostress determinations will be proposed. The results will be checked against a purely geometrical attempt for retrodeforming the movement along the Engadine line.

2. Determination of movement vectors using fault rock data

a. Fault rocks of the master fault

There are only very few outcrops of the master fault since its trace is mostly covered by alluvials. Good exposures are found at two localities only. The first is near Maloja pass, in particular in the creek bed of the Orlegna near Orden, 1 km SE of Maloja pass. These outcrops have been described by Mützenberg (1986) and Liniger (1992) and consist of unfoliated cataclasites. These cataclasites do not allow for the determination of a movement vector since striations and sense-of-movement criteria are absent. Mützenberg (1986) inferred the movement direction from drag folds, assuming the

movement direction to be perpendicular to the fold axis of such drag folds. This method can lead to erroneous deductions since the orientation of drag folds also crucially depends on the pre-existing orientation of the folded layer in respect to fault plane and movement vector. In spite of this, his inference, a sinistral strike-slip component, combined with relative uplift of the SE block, was confirmed by Liniger (1992), who measured lineations within subsidiary faults immediately south of and parallel to the master fault which is in a vertical orientation here. Sense-of-shear criteria allow the determination of a movement vector dipping between 50–62° towards the SW.

Secondly, good outcrops of the Engadine line occur at the Stragliavita pass near Zernez, where fault gouges predominate within the sediments of the Engadine dolomites, while the Silvretta basement rocks contain cataclasites with a weakly developed stretching lineation and limited amounts of crystal plasticity affecting quartz domains. Here the lineation within the cataclasites exhibits a 60° pitch towards the E within the foliation plane parallel to the trace of the master fault, dipping with about 45° towards the SE. This, together with sense-of-shear criteria, indicates a combined sinistral and normal-fault (SE side down) movement at Stragliavita pass.

b. Method of stress determination using minor fault populations near the master fault

Because only very little information can be gained from investigations concerning the master fault as such, attention was drawn to minor faults in the immediate neighbourhood of and related to the activity of the master fault. However, the affiliation of mesoscopic faults producing minor offsets in the cm to m range to the activity of the master fault has to be demonstrated. An increasing density of minor faults towards the master fault, established by careful profiling perpendicular to the trace of the master fault, was used as the main argument for regarding the analysed minor faults as being related to movement along the master fault.

Table 1 lists the six localities used for fault population analysis. Five of these localities are actually situated along the Engadine line as such while locality 6 is situated along a

Table 1: List of analysed localities

locality nr.	area	average Mohr angle
locality 1 Stragliavita pass	basement and cover rocks at 2200–2700 m S of Stragliavita pass	20°
locality 2 Punt Nova	basement along road cut near Punt Nova bridge 800875/172675	24°
locality 3 Val Mela	basement and cover in the area between Val Mela and Val Torta near Cinuos-chel	25°
locality 4 Samedan	road cut NE of Samedan 787400/157500	20°
locality 5 Maloja	basement in area S and SE of Maloja pass: Orden and Piz L'Aela	22°
locality 6 Piz Mezzaun	Raibl beds along Mezzaun normal fault north of Piz Mezzaun 793300/161300	25°

normal fault (Mezzaun normal fault) which we initially considered to be directly related to movements along the Engadine line.

The fault population analysis served to determine the orientation of the principal stress axes active at the time of formation of these minor faults. At localities 1, 2, 3, 4 and 6 individual fault planes and/or conjugate sets of fault planes and associated slickensides with unequivocal sense-of-shear indicators (exclusively fibre-growth slickensides, see Means 1987) were used. At locality 5 no slickensides were available and the stress determination is entirely based on measuring conjugate Mohr type fractures, a complementary approach also used for a minor part of the data sets of the other localities. The arithmetic mean of the Mohr angles as measured at each locality is given in Table 1 and varies between 20° and 25°.

Basically there are two different approaches in paleostress determination. The dihedron method (i.e. Angelier & Mechler 1977, Pfiffner & Burkhard 1987) assumes that the distribution of fault planes and the stress reactivating such fault planes are independent. This method searches for an optimal orientation of the stress deviator which is capable of reactivating pre-existing discontinuities. In theory this method is also capable of deriving stress ratios (parameter φ of Angelier 1979), or perhaps more adequately, ratios of principal strains, since the discontinuities are merely reactivated in order to produce strain. Following this method, σ_1 (the maximum compressive stress axis) may lie anywhere within a compressive dihedron. The other approach is to directly deduce the orientation of the principal stress axes from the orientation of minor faults. This approach was chosen in the present analysis. By measuring the Mohr angle (an average was used for each locality, see Table 1) the orientations of the axes of principal stresses were determined for each individual fault plane or conjugate fault set. The reasons for choosing this approach are the following: (1) only newly formed fractures with minor offset were used and hence it is appropriate to interpret these faults as being caused by a given stress tensor, (2) the ultimate goal of the analysis was the determination of stress axes and not strain axes as is the fact in case of the dihedron method in our opinion, (3) we were not interested in determining "stress ratios" (see second point), the main "advantage" of the dihedron method, because we do not share the view that stress ratios remain constant in time.

From the determined stress axes, mean orientations of the principal stress axes were statistically determined for each locality. In a second step, the principal stresses were resolved onto the orientation of the master fault. Because the stress ratio remains unknown this leads to a range of possible movement directions within the master fault. The basic assumption of our method is that minor fault populations record the orientations of the principal stress axes present during movements along the pre-existing master fault.

Figure 2 illustrates the method used for the case of locality 2. Direct inspection of the raw data (Figs. 2a and b) makes it clear that both normal and strike-slip faults are present, a feature representative also for the other localities. No systematic age relationship between the two populations can be derived in the field. This illustrates the fact that there must have been repeated changes in the relative magnitude of horizontal and vertical stress axes (see discussion in Laubscher 1972). In this case σ_3 remained constant while σ_1 and σ_2 were repeatedly exchanged (σ_2 subvertical for strike-slip faults, σ_1 subvertical for normal faults). In terms of strain this leads to an overall constriction of the material affected by minor faulting.

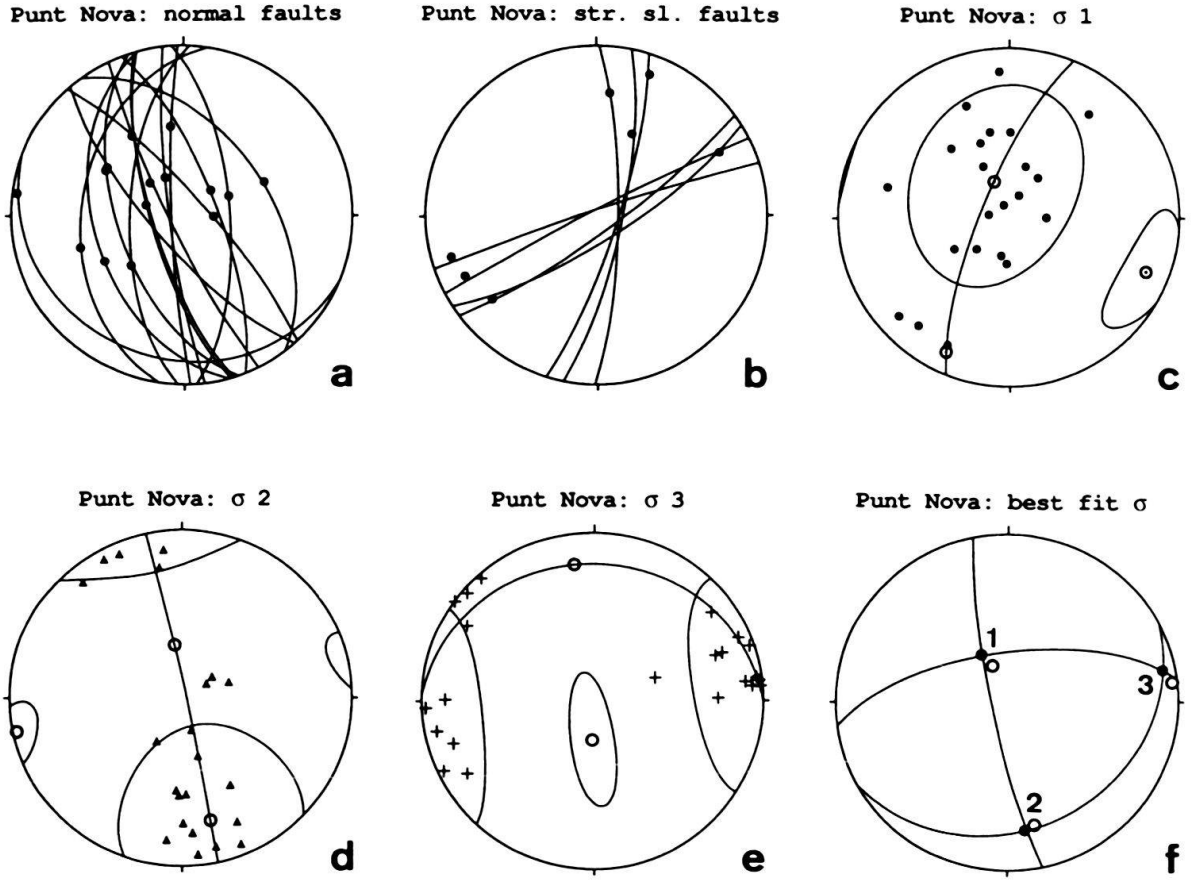

Fig. 2. Determination of the mean directions of principal stress illustrated for the measurements at locality 2 (Punt Nova, see Table 1). a, b: fault planes and slip vectors of normal and strike-slip faults. c, d, e: Bingham statistics performed separately for each of the three axes of principal stress, evaluating the three orthogonal eigenvectors and elliptical cones of confidence (0.95) around the first and third eigenvector. f: compilation of the first eigenvectors from Figs. 2c, d, e (estimate of the distribution mean for the three principal stress directions, open circles) and minor adjustments needed for having these independently determined eigenvectors orthogonal (full circles).

In principle the next step in the analysis is just as questionable as the method of Angelier & Mechler (1977) in that an attempt is made to determine the principal directions of an average stress tensor in spite of the fact that reality is undoubtedly more complex. This was done by determining (individually for each of the three principal axes of stress; Figs. 2c, d, e) the three orthogonal eigenvectors of the orientation tensor for an orthogonal Bingham distribution (program Stereoplot kindly provided by Manck-telow 1989, mathematical treatment based on Cheeney 1983). This results in the three stress axes being almost perpendicular to each other (open circles in Fig. 2f) and only minor trial and error adjustments were necessary for making them exactly orthogonal (filled circles in Fig. 2f).

In a further step a range of possible slip vectors within the master fault was derived by finding the maximum resolved shear stress of the mean stress tensor within the plane of the master fault. This range results from the fact that the direction of the maximum resolved shear stress depends on the unknown stress ratio. The range depicted in the stereograms contained in Fig. 5 and Plate 1a incorporates all the extremes between

uniaxial compression and uniaxial extension (see Fig. 4 in Angelier 1979). For uniaxial compression the direction of maximum resolved shear stress is found by intersecting the great circle containing the fault plane normal and σ_1 with the fault plane, for uniaxial extension σ_1 is replaced by σ_3. The resulting spread also depends on the orientation of σ_2 and is zero if σ_2 is contained within the master fault (this is the case at locality 4, see Plate 1 a).

Of course the method used stands and falls with the inherent assumptions, namely (1) the existence of an average stress tensor and (2) that this average stress tensor recorded in the minor faults may be resolved onto the pre-existing master fault in order to yield a movement vector. The correctness of these assumptions will be evaluated at a later stage, the next section first discusses the results regarding all the localities.

c. Results of the stress analysis using minor fault populations

Fig. 3 depicts the orientations of the principal stress axes as derived for the 6 localities listed in Table 1. Localities 1–3 situated between S-chanf and Stragliavita pass (Plate 1 a) were collected along that part of the Engadine line which exhibits a moderate inclination towards the SE (contours of the Engadine line in Plate 1 a). At all the 3 localities σ_3 is subhorizontal and E to ESE oriented (Figs. 3 a, b, c, i). The σ_1 axes have a great circle distribution around σ_3, however with a tendency to form a maximum around a subvertical to steeply N-dipping direction (Figs. 3 a, b, c, g). This implies frequent changes between normal fault and strike-slip fault and hybrid modes with a preference for normal faulting. The patterns are very similar for individual localities (Figs. 3 a, b, c) and consequently the best-fit procedure for finding an average stress tensor and resolving that stress tensor onto the master fault (Plate 1 a) yields similar results for localities 1–3.

The range of possible pitches of the inferred movement direction is between 26 and 73° towards the E taking into account all the localities 1–3. The resulting sense of movement is in agreement with the inferences drawn from the cataclasites collected at the Stragliavita pass locality. The orientation of the lineation contained within these cataclasites (60° pitch) is within the range of pitches deduced from the stress analysis method. Hence, according to the method used, the kinematics inferred for the Stragliavita pass area are representative for the entire SE-dipping portion of the Engadine line between Stragliavita pass and S-chanf: sinistral strike-slip combined with downfaulting of the Engadine dolomites in respect to the Silvretta basement.

Two possibilites for the SW-ward continuation of the Engadine line as observed in the Lower Engadine ("Stragliavita line") beyond S-chanf are feasible. A first one is to search for a continuation at the base of the Languard-Ortler units and along the Mezzaun normal fault (locality 6, Table 1). In this case the "Stragliavita line" would be unrelated to the Engadine line of the Upper Engadine ("Maloja line"). A second one is to directly connect the Engadine line of locations 1–3 with the Engadine line as exposed between Samedan and Maloja (localities 4, 5). The results for locality 6 (Fig. 3 f, insert of Fig. 5) indicate that σ_1 and σ_2 are well separated, σ_1 being subvertical and σ_2 horizontal. This is different from localities 1 to 3 ("Stragliavita line") were σ_1 and σ_2 are often interchanged. Additionally, the range of possible movement directions obtained by resolving the average stress tensor onto the Mezzaun fault is between dextral strike-slip and top-SW directed normal faulting, which is incompatible with the movement direc-

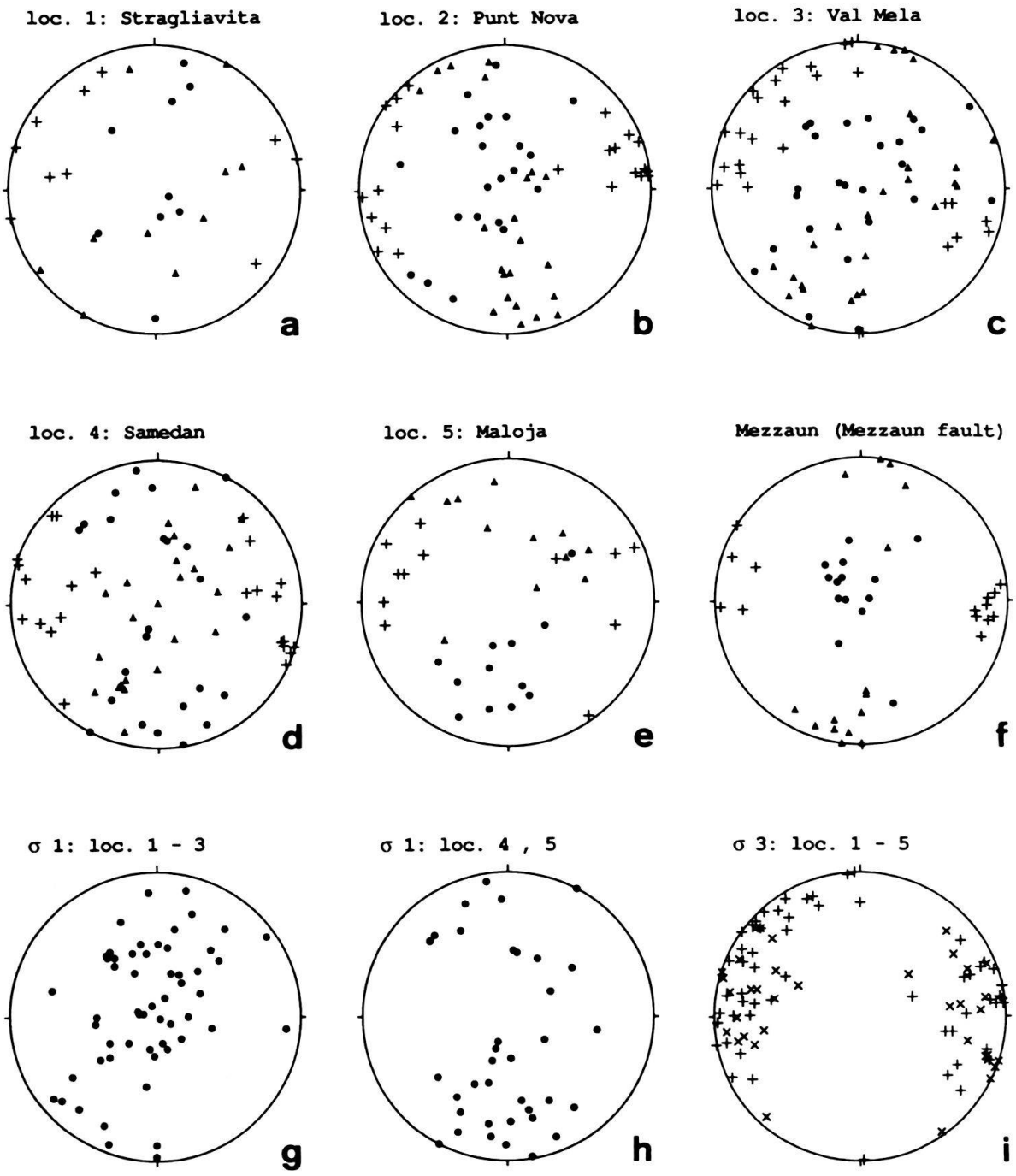

Fig. 3. Compilation of the results of the paleostress analysis for 6 localities (Table 1). a–f: orientation of σ_1 (dots), σ_2 (triangles) and σ_3 (crosses) obtained at each locality. g, h: compilation of the orientation of σ_1 for the NE (g) and SW (h) part of the Engadine line. i: σ_3 at localities 1–3 (vertical crosses) and 4–5 (diagonal crosses).

tions obtained from localities 1–3. This favours the second possibility (continuation of the "Stragliavita line" into the "Maloja line"). Other arguments favouring this view will be discussed in a later section.

The orientation of the master fault, for the time being considered to follow the valley floor, cannot be inferred by contouring SW of S-chanf. A subvertical orientation was

assumed at Samedan (locality 4), based on the findings between Maloja and Stampa, where intersection with topography again allows for an exact determination of the inclination (vertical to very steeply N-dipping). At localities 4 and 5 σ_3 is again oriented E–W (Figs. 3d, e, i), figure 3i (diagonal crosses) suggesting a slightly different orientation in respect to localities 1–3 (the latter have more SE–NW-oriented σ_3). Again, σ_1 straddles a great circle around σ_3 (Fig. 3h), however at locality 5 in isolation (Fig. 3e) an inclination of σ_1 towards the S is clearly preferred. Resolving the mean stress orientations onto the master fault yields pure sinistral strike-slip motion at Samedan and sinistral strike-slip combined with uplift of the SE block at Maloja. The deduced movement direction dips between 12 and 56° to the SW at Maloja. This is at least qualitatively in agreement with the inference of Liniger (1992) regarding the orientation of the movement vector and is in perfect agreement regarding the sense of shear inferred by both Mützenberg (1986) and Liniger (1992).

In summary, regarding localities 1–5 as being situated along a throughgoing single Engadine line, a rather complex combination of movement vectors may be inferred from the paleostress analysis. A sinistral strike-slip fault with extensional downfaulting of the SE block in the Lower Engadine would grade into a pure strike-slip fault at Samedan, finally producing an opposite vertical component at Maloja with vertical uplift of the SE block.

Additional interesting features result from the stress analysis. At all the localities except locality 4 the mean orientation of σ_1 tends to make a surprisingly large angle in respect to the master fault ($>45°$), while σ_2 is not contained within the master fault. Hence the stress field in the neighbourhood of the master fault recorded in the minor fault population is not responsible for the creation of that master fault. The high-angle orientation of σ_1 in respect to the master fault is compatible with a very low strength of the material near the master fault (see discussion by Zoback et al. 1987, and Mount & Suppe 1987 regarding the San Andreas fault). Another feature concerns the strain produced by minor faulting within the wall rock near the master fault: exchange between σ_1 and σ_2 with fixed σ_3, typical for localities 1–5, suggests constrictional deformation (or, alternatively, a value of φ near 1 if one prefers to argue in terms of stress).

3. Determination of the movement vector using large scale nappe correlations

By using large scale nappe correlations across the Engadine line the possible movement vectors may be further constrained and the validity of the assumptions underlying the deduction of the movement vector based on paleostress analysis may be discussed. This correlation of tectonic units is well constrained for the region between Stampa and St. Moritz (Liniger & Guntli 1988, Liniger 1992). Northeast of St. Moritz, however, nappe correlations are a matter of debate and in fact at least partly depend on the knowledge of the movement vector rather than serving to constrain this vector.

By correlating intersection points of planar surfaces or major hinge lines of folds the movement vector may be determined. Unfortunately this method is impracticable for our area of interest. Consequently, a trial and error retrodeformation of major nappe contacts between Stampa and St. Moritz was attempted, encouraged by the fact that not all

nappe contacts are plane parallel. In a first step major nappe contacts (labelled 1–8 in Plate 1 a) were contoured. Our own data (mainly concerning the Engadine line and nappe contact 8, i.e. the base of the Upper Austroalpine units) were complemented with data from Cornelius 1932, Bearth et al. 1987, Liniger 1992, Staub 1921, 1946. In a second stage, a vertical cross section parallel to the Engadine line was constructed between Vicosoprano and S-chanf (Plate 1 b) by using the contour data of Plate 1 a in order to constrain the lines of intersection of the nappe contacts with the plane of the profile.

It has to be emphasized that the version pictured in Plate 1 b was arrived at solely by considering nappe contacts 1–6. Regarding nappe contacts 1 and 2 NW of the Engadine line, usage of the intersection line resulted in geometrical impossibilites. Consequently, the topology of these nappe contacts near the Engadine line was attributed to drag folding. Plate 1 b therefore depicts the intersection of the nappe contacts 1 and 2 as constructed by linear extrapolation of the contour lines at some distance from the master fault (dashed contours in Plate 1 a). For all the other nappe contacts rigidity of the country rocks to both sides of the master fault was assumed. Hence the retrodeformation pictured in Plate 1 b is qualitatively fully constrained by nappe contacts which may be unambiguously correlated across the master fault. Further constraints on the exact version in Plate 1 b are given by the fact that the base of the Upper Austroalpine Languard nappe only occurs SE of the Engadine line. Hence at this point along the profile the sense of the vertical displacement component must already have been reversed in respect to the situation at Maloja pass. This constrains the point of no vertical offset to be searched for somewhere between Samedan and St. Moritz (i.e. between the base of the Languard nappe labelled 8 E of St. Moritz and nappe contact 6, the base of the Bernina-Julier nappes SE of the Engadine line in Plate 1 a).

The nappe correlation proposed in Plate 1 b suggests a 4 km long movement vector plunging 45° to the SW at Maloja pass producing a sinistral strike-slip component combined with relative uplift of the SE block (2.8 km each). This estimate is qualitatively in agreement with the estimates of Liniger & Guntli (1988) and Mützenberg (1986). The 45° plunge of the vector is within the range predicted from the paleostress analysis (12–56°) and somewhat shallower than the lineations measured by Liniger (1992) which plunge 50–62°.

Between St. Moritz and Samedan a horizontal sinistral movement vector is indicated and this is in perfect agreement with the paleostress analysis at locality 4 near Samedan. A 4.5 km long NE plunging (45°) movement vector is predicted near S-chanf, the vertical component (3.2 km) being reversed in respect to the situation at Maloja. Again, there is good agreement with the paleostress data from localities 1–3. Additionally, the retrodeformation fits with the orientations of the lineations within the cataclasites at Stragliavita pass and the deduced sense of shear at this locality. Note, however, that the Engadine line is no longer vertically oriented at and NE of S-chanf (Somm 1965 and contours given in Plate 1 a). For simplicity the retrodeformation in Plate 1 b only treats movements within a vertical plane. Of course, such a change in orientation of the fault plane must be accompanied by internal deformation within the country rock.

Mutual agreement between this retrodeformation on one hand and inferences drawn from the paleostress analysis and the few data concerning the fault rocks of the master fault on the other hand strongly suggests that: (1) there is in fact one single Engadine line as proposed by Trümpy (1977), (2) that there is no transformation of strike-slip move-

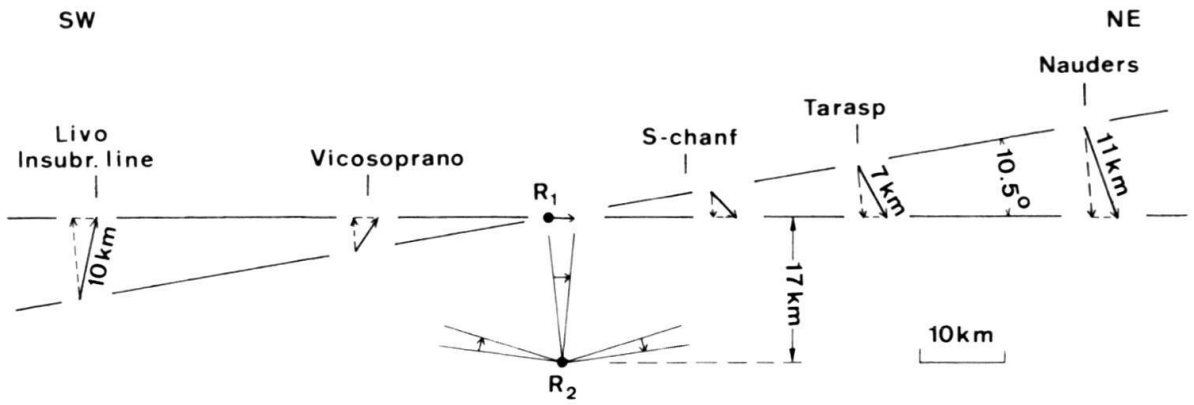

Fig. 4. Scheme exploring possible consequences of the block rotation model. Note that block movement and rotation may be described by a single stationary rotation axis (R_2, solid vectors) or, alternatively, by any combination of translation and rotation (R_1 illustrates the case of a rotation axis at the earth's surface, broken vectors add up to give the vector resulting from R_2).

ment into thrusting or folding within the wall rocks which can be assumed to remain rigid to a first approximation, and, (3) that the assumptions behind using the paleostress analysis for determining the movement vector may be correct.

Fig. 4 seeks to explore the consequences resulting from such a model of oblique slip and rotation of two rigid blocks. The movement of the SE block in respect to the NW block may be described as a rotation around a stationary rotation axis at a depth of 17 km below Samedan. Alternatively, a horizontal movement of a simultaneously active rotation axis, for example situated at the earth's surface, may be envisaged. Both scenarios result in an identical velocity field and there are no data to decompose this velocity field. It is clear that this rigid block model is bound to break down at a certain depth (at the brittle-ductile transition) and also laterally (vertical component of displacement cannot increase indefinitely).

If we assume that the rigid block model is also valid outside the area of investigation (i.e. SW and NE of the area covered by Plate 1) and that the fault plane remains vertical, a nearly vertical displacement vector of about 10 km would result at a putative intersection point of the Engadine line with the Insubric line near Livo (immediately W of the northern end of Lago di Como, Fig. 4). In fact, there is no continuation of the Engadine line in the sense of a discrete fault W of Valle della Mera. The transition from discrete movement along the master fault into distributed strain within the country rock (so-called brittle-ductile transition) is very likely for the SW continuation of the Engadine line in Val Bregaglia (Wenk 1984). Further work is needed in order to trace such a zone of intense ductile shearing. The northern part of the Gruf complex and/or the contact between Gruf complex and Chiavenna ophiolites (Schmutz 1976) are the most likely candidates. In fact, there is a very high metamorphic gradient across Gruf complex and Chiavenna ophiolites (Schmutz 1976, Bucher-Nurminen & Droop 1983), suggesting fast and substantial relative uplift of the Gruf complex (see Fig. 17 in Bucher-Nurminen & Droop 1983). If coeval, this uplift is compatible with the predictions from Fig. 4.

In regard to the NE continuation of the Engadine line, Fig. 4 predicts increasing vertical offset by downfaulting of the SE block (Engadine dolomites). Near Tarasp (western end of the Engadine window) the vertical component would amount to about

6 km. A profile construction across the Engadine line (Schmid & Haas 1989, Fig. 5b) requires an absolute minimum vertical offset of 3 km at this locality. Assuming the base of the Austroalpine nappe stack to be another 3 km below the basement-sediment interface within the Engadine dolomites, a total of 6 km offset could in fact be deduced from this profile. The prediction of increasing offset towards the NE (about 10 km around Nauders) is not unrealistic either because the map pattern (Fig. 1) shows that the base of the Oetztal nappe (Schlinig thrust) almost merges with the Engadine line near Nauders. There the next higher Oetztal nappe is almost directly juxtaposed with the Penninic units of the Engadine window, the Engadine Dolomites exhibiting a strong axial plunge towards the NE and below the Oetztal unit. Additionally, the Schlinig thrust changes its orientation from a NW–SE strike (Schmid & Haas 1989) into a N–S (Stutz & Walter 1983) and finally a SW–NE strike, subparallel to the Engadine line near Nauders. Stäuble (1987) inferred a 52° dip toward SE for the Schlinig thrust at Piz Lad near Nauders from contour mapping. This present-day geometry of the Schlinig thrust may be interpreted as being due to larger scale drag folding of a pre-existing thrust of Cretaceous age (Thöni 1986), caused by the combined effect of updoming of the Engadine window and downfaulting of the SE block along the Engadine line during the Tertiary.

The further continuation of the Engadine line NE of Nauders (E of Fig. 1, see Fig. 6) remains a puzzling problem. According to Oberhauser (1980), Thöni (1980) and Mattmüller (1991), the Oetztal unit eventually comes into direct contact with the Engadine window. These authors held late W-directed thrusting of the Oetztal nappe onto the Engadine window to be responsible for displacing the pre-existent Engadine line. Large-scale considerations also indicate thrusting of the frontal Oetztal nappe to the N and NW onto Engadine window, Silvretta nappe and Northern Calcareous Alps (Ratschbacher et al. 1991 b). Such late thrusting of the frontal Oetztal unit could in fact be contemporaneous and linked with the middle to late Miocene activity along the sinistrally transpressive Giudicarie belt (Laubscher 1990). Alternatively, the map pattern could also be interpreted to be caused by normal (low-angle) faulting along the Engadine line, continuing beyond Nauders. Unfortunately no sense-of-shear indicators regarding the contact between Oetztal nappe and Engadine window are available so far.

At this point we want to re-emphasize that Fig. 4 merely explores possible consequences of the rigid block rotation model. While this model explains the movements along the Engadine line reasonably well between upper Val Bregaglia and Nauders, it is obvious that the vertical component cannot increase indefinitely towards the NE. Apart from the possible effects of later overprinting discussed above, simultaneous deformation of the blocks bounding the Engadine line may eventually lead to movement vectors departing from those predicted by Fig. 4. Returning to the area investigated, there are in fact indications that at least the SE block has not behaved rigidly during movements along the Engadine line. In Plate 1a some major normal faults within the Engadine dolomites have been contoured (labelled b, c, d, e in Plate 1a). The exact movement vector and age of these normal faults are still unknown. However, the orientation of the normal faults in respect to the orientation of σ_3 (Plate 1a) suggests dextral transtension. This is especially indicated for the steep fault labelled e in Plate 1a (Chavagl fault): the local change in strike and dip of the Engadine line SE of Zernez coincides with the intersection area of the two faults, suggesting simultaneous activity. Simultaneous activ-

ity of dextrally transtensive faults and the sinistrally transtensive Engadine line E of S-chanf would imply E–W extension within the SE block (Engadine dolomites). As mentioned earlier internal deformation within the country rocks is also predicted by the change in inclination of the Engadine line near S-chanf, from a vertical into a SE-dipping orientation.

In conclusion, the rigid block model of Fig. 4 probably does no longer hold SW of Val Bregaglia (increasingly ductile deformation) nor NE of Tarasp (simultaneous deformation within the blocks bounding the Engadine line). Between Val Bregaglia and Tarasp, however, it provides a first order approximation for the displacement vectors. This first order approximation may be refined in the future by a quantification of simultaneous deformation within the blocks and/or by additional information on the direction of the displacement vectors outside the area covered by Plate 1.

4. Nappe correlations across the Engadine line NE of St. Moritz

While well-established nappe correlations in the upper Engadine served as input for the retrodeformation depicted in Plate 1 b, the consequences of such a model for less obvious correlations NE of St. Moritz will be discussed in this chapter. Fig. 5 depicts two profiles constructed along a trace running parallel to and close to the Engadine line (NW and SE of the line, location in Fig. 1). These profiles do not correlate at all, supporting the earlier conclusion that the Engadine line as seen near Maloja in fact continues directly into the lower Engadine. The SE side (Fig. 5 b) is characterized by the broad antiform of the Mezzaun half-window, while units on the NW side (Fig. 5 a) uniformly dip to the N or NE. The profiles were also used to construct the large scale configuration pictured in Plate 1 b.

Plate 1 b clearly shows that the widely accepted view that Julier and Bernina nappes may be directly correlated is confirmed. The same can be said for the correlation between Grevasalvas and Corvatsch units. Plate 1 b suggests that the latter correlates with the Err nappe further to the NE. A first surprising feature of Plate 1 b is the extreme thinning of the Julier-Bernina nappe near Samedan. Tentatively, the thinning is attributed to low angle normal faulting within the Samedan zone, predating movements along the Engadine line. Normal faulting has recently been recognized to be very widespread within the western Austroalpine units of Graubünden. A first episode is inferred to be of Late Cretaceous age (e.g. Corvatsch mylonite zone and Ducan normal fault; Liniger 1992 and Froitzheim 1992). A second one is of Tertiary age (e.g. Turba mylonite zone; Nievergelt et al. 1991, Liniger 1992).

NE of Samedan the Julier-Bernina nappe has been eroded NW of the Engadine line but finds its continuation into the Mezzaun sedimentary unit SE of the Engadine line. The stratigraphic basement of this Mezzaun unit is at subsurface next to the Engadine line but exposed in form of the Stretta unit, a higher digitation of the Bernina nappe, at some distance away from the Engadine line. Additionally, basement and cover of the Corn slice (Fig. 5 b) may be considered as detached elements of the Bernina nappe. The Languard nappe at the base of the Upper Austroalpine nappe pile exhibits a broad synform, striking E–W (Plate 1 a).

According to Plate 1 b the Seja basement has to be correlated with the Err nappe. Hence, the direct contact between Seja basement (Err) and Mezzaun sediments (Bernina)

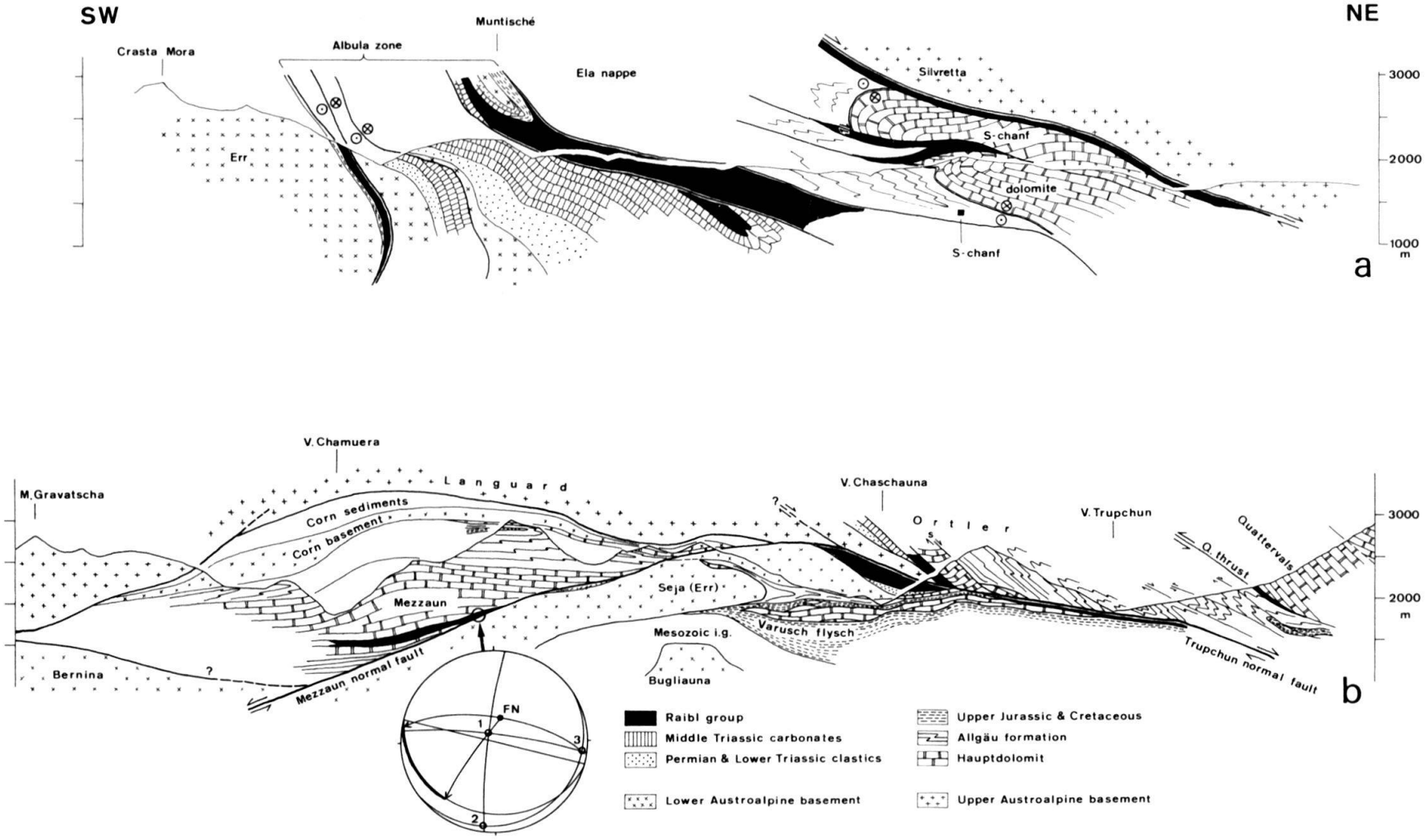

Fig. 5. Profiles constructed parallel to the Engadine line NE of Samedan (traces in Fig. 1; 5a situated NW of and 5b SE of the Engadine line). The profiles cannot be correlated across the valley floor without invoking substantial movements along the Engadine line (discussion in text). The results of the paleostress analysis performed at locality 6 (Table 1) are inserted in the form of a stereoplot (legend for reading the stereoplot see Plate 1).

is formed by a fault of considerable importance: the Mezzaun normal fault. The paleostress analysis at locality 6 (inset in Figure 5b) suggests downfaulting of the hangingwall (Julier-Bernina unit) along the Mezzaun fault towards the SW or W above the footwall (Err unit). There is no additional information, however, regarding the sense of shear along this normal fault and top to the E downfaulting cannot completely be excluded (note that σ_1 makes a very small angle in respect to the fault plane normal, see inset of Fig. 5b). This Mezzaun fault may possibly be directly connected with the normal fault at the base of the Samedan zone, being offset by the Engadine line (contours labelled "7" in Plate 1a). This normal faulting is tentatively interpreted to be of Late Cretaceous age.

The most important consequence of the retrodeformation proposed concerns the position of the Ela nappe. This nappe appears in a very low structural level in respect to the base of the Upper Austroalpine nappe system on the other side of the Engadine line (Languard nappe). Hence its position is definitely Lower Austroalpine. Such a view is independently supported by the very close facies analogies between Ela nappe and Mezzaun unit during the Early and Middle Jurassic (Eberli 1988). Structural arguments suggest that the sediments of the Corn unit (immediately overlying the Mezzaun unit, Fig. 5b) represent the direct continuation of the Ela nappe across the Engadine line. Although the Ela nappe directly lines up with the sediments of the Ortler zone in map view (possibly the reason for attributing the Ela nappe to the Upper Austroalpine by all previous workers), both units occupy very different tectonic levels. This is again independently supported by illite crystallinity data, indicating a markedly lower metamorphic grade for the westernmost Ortler zone, when compared to the Ela nappe (preliminary data by P. Conti, pers. comm.). Additionally, the incompatibility of the profiles depicted in Fig. 5, particularly at their SW end, prevents any direct correlation in map view across the Engadine line.

The internal structure of the Err nappe, Albula zone, Ela nappe, S-chanf Dolomite, Mezzaun unit and Corn slices is extremely complex due to post-nappe refolding, associated with vertical shortening and accompanied by normal faulting restricted to higher structural levels during the Late Cretaceous, as discussed elsewhere (Froitzheim 1992). Facies analogies and structural arguments suggest a continuation of the Ela nappe into the Mezzaun and Corn units (Julier-Bernina nappe s.l.). Such a correlation would imply large scale post-nappe refolding of the Julier nappe s.l. (Mezzaun-Corn-Ela units) around the front of the Err-Seja basement, as suggested by the geometry evolving from Plate 1b and similar to well-documented structures NW of the Engadine line (Froitzheim 1992).

A surprising feature of Plate 1b is that the basal contacts of the Upper Austroalpine nappes to both sides of the Engadine line (base Silvretta nappe and base Ortler zone) line up along a single N-dipping plane (see contours in Plate 1a). According to Froitzheim (1992) this dip to the N is due to late stage open folding (local f3 in the Ela nappe) redeforming earlier Late Cretaceous post-nappe folds and associated normal faults (local f2 in the Ela nappe). Due to the fact that the slip vector along the Engadine line runs at a small angle to the intersection line between the base of the Upper Austroalpine units and the fault plane corresponding to the Engadine line, only insignificant offset results in the map pattern (a small apparent dextral offset is visible in map view, Fig. 1). The updoming of the Mezzaun half window is possibly a combined effect of late open folding (local f3) and extensional unroofing (local f2) and certainly predates movements along the Engadine line.

There is an important difference, however, regarding the lithology of the rocks near the basal thrust plane of the Upper Austroalpine units to both sides of the Engadine line. NW of the line an impressive volume of basement rocks is found (Silvretta basement). However, the basal thrust of the Silvretta basement (WNW movement) has been reactivated as an ESE-directed normal fault in the Late Cretaceous (Ducan normal fault, Froitzheim 1992). Hence the original nappe pile was already dissected prior to movements along the Engadine line. On the SE side, the base of the Ortler zone is almost devoid of Upper Austroalpine basement and was reactivated by the Trupchun normal fault (Fig. 5b). Moreover, this Trupchun normal fault directly juxtaposes the sediments of the Ortler zone with the Varusch flysch (Fig. 5b), also omitting the higher units of the Lower Austroalpine (e.g. Corn slice and Mezzaun unit, equivalents of the Julier-Bernina nappe). The movement vector of the Trupchun normal fault is not known due to poor outcrop conditions. It may be at a considerable angle relative to the plane of the section producing the peculiar geometry depicted in Fig. 5b. Tentatively, we relate normal faulting along the Trupchun normal fault to the activity along the Ducan normal fault, although a direct geometrical connection, as suggested by the line-up in Plate 1b, is uncertain.

If we assume top-E normal faulting along the Trupchun normal fault (interpreting the Trupchun normal fault as the direct continuation of the Ducan normal fault) and top-W movement along the Mezzaun normal fault (based on the paleostress analysis, see inset of Fig. 5b), Mezzaun and Trupchun normal faults appear as conjugate normal faults to both sides of the Mezzaun half window contoured in Plate 1a (as drawn in Plate 1b and Fig. 5). For simplicity the profile of Fig. 5b depicts the base of the Upper Austroalpine units (Languard nappe and Ortler zone) as a single surface, well constrained by the contours of Plate 1a. It has to be emphasized, however, that the sense of shear (top W, as indicated in Plate 1b and Fig. 5b) regarding normal faulting along the Mezzaun fault and the Samedan zone is not well constrained and top-E movement along both normal faults cannot be excluded. Local f3 folding may have substantially overprinted an older, Late Cretaceous top-E normal faulting geometry, resulting in a complicated outcrop pattern. Hence, the geometry of Late Cretaceous normal faulting is not yet fully understood, except for the Ducan normal fault (Froitzheim 1992).

While the reconstruction shown in Plate 1b does not allow for the deduction of the exact geometry and kinematics regarding the complicated Mezzaun half window, conclusions may be drawn regarding mutual relationships between the various Upper Austroalpine thrust sheets on a larger scale. Languard and Silvretta nappe can be directly correlated in the sense that both units represent the base of the Upper Austroalpine nappe system. The Silvretta nappe, being substantially uplifted NW of the Engadine line, comes to lie below Ortler zone and Engadine Dolomites after retrodeformation (Plate 1b). Hence, the Silvretta nappe NW of the Engadine line may easily be correlated with the Sesvenna basement (stratigraphic base of the Engadine dolomites), the vertical throw increasing towards the NE as discussed in an earlier chapter. While the correlation Languard-Silvretta-Sesvenna appears certain, some questions regarding the position of the basement slivers stratigraphically in contact with the Ortler zone, preserved to the E of and at some distance from the Engadine line, and the position of the Campo basement remain open at this stage. Work in progress (Conti pers. comm.) suggests a major W-directed thrust between Ortler zone (sediments and thin basement slivers such as

found at Alpe Trela (Pozzi & Giorgelli 1960)) and Campo basement along the so-called Zebru line. In summary, the original Upper Austroalpine Languard-Silvretta-Sesvenna basement formed the base of the upper Austroalpine nappe system, dissected both by Cretaceous normal faulting, locally omitting the basement altogether (Trupchun normal fault) and Late Tertiary movements along the Engadine line.

5. Discussion and conclusions

On a large scale and in map view (Fig. 6) the Engadine line appears as a conjugate strike-slip fault in respect to the Tonale line, an E–W running segment of the Periadriatic line (Schmid et al. 1989). The angle forming the releasing intersection, however, is 45° or less, not confirming with Mohr-Coulomb theory at first sight. Two reasons may account for this: first both lines are not pure strike-slip faults but have transpressive (Tonale Line, Schmid et al. 1989) or transtensive (NE Engadine line) elements, secondly, boundary

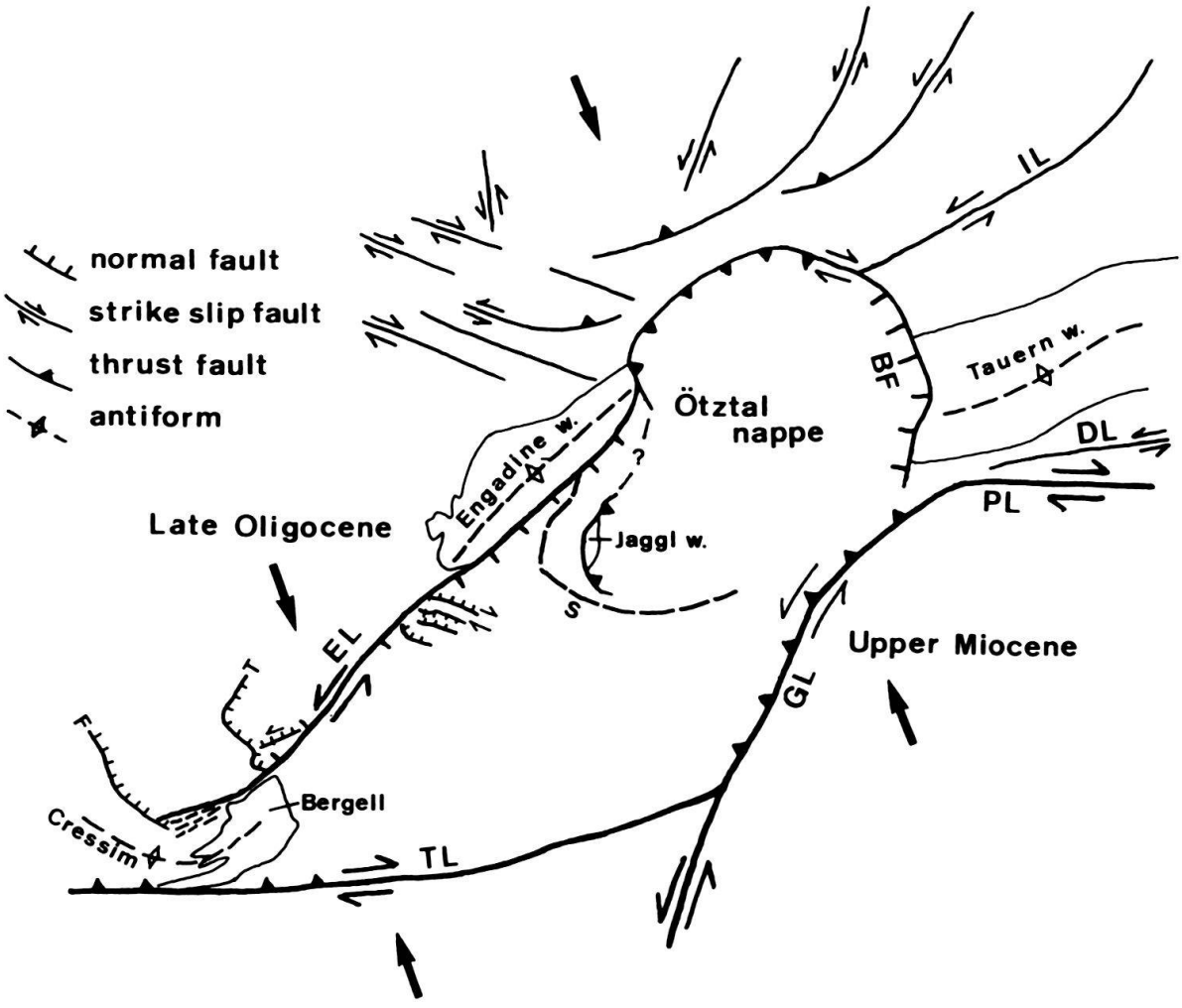

Fig. 6. Sketch map illustrating geometric relationships with other Late Oligocene to Miocene post-collisional structures found in the surrounding areas (partly after Ratschbacher et al. 1991 b). EL: Engadine line; TL: Tonale Line; GL: Giudicarie line; PL: Pustertal line; DL: Defereggen-Anteselva-Vals line; IL: Inntal Line; BF: Brenner fault; S: Cretaceous thrust at base of Oetztal nappe (Schlinig thrust); F: Forcola normal fault; T: Turba mylonite zone.

conditions and kinematics of progressive deformation may modify the orientation of early nucleated faults (see Ratschbacher et al. 1991 a, Fig. 4).

The western part of Fig. 6 depicts some structures which are inferred to be roughly contemporaneous with movements along the Engadine line during the Late Oligocene to Early Miocene. Two prominent normal faults indicate E–W extension at the E margin of the Lepontine dome: the Forcola line (at the base of the Tambo nappe, Weber 1966), possibly synchronous with the Engadine line, and the Turba mylonite zone, predating the Engadine line and the Bergell granodiorite intrusion (30 Ma, von Blanckenburg 1992). At the same time the Cressim antiform (Heitzmann 1975) indicates N–S compression believed to be partly contemporaneous (work in progress) with the Novate intrusion (26 Ma, Köppel & Grünenfelder 1975) and hence affecting the already emplaced Bergell intrusion (the same can be said for the backthrusting stage along the Tonale line). Hence N–S compression resulted in folding and uplift of the Bergell area and roughly contemporaneous E–W extension N of the Bergell area.

At this stage some clarifications concerning nomenclature are indicated. Firstly we emphasize that in our usage the term "extension" merely means a stretch of a horizontal datum plane parallel to a particular direction and does not necessarily imply crustal thinning. Secondly extension may occur during converging motions. Recently Ratschbacher et al. (1991 a, b) proposed the term "lateral extrusion" for strike-parallel, E–W directed extension in the Eastern Alps, combined with lateral escape along strike-slip faults as a result of N–S convergence or compression. According to these authors lateral extrusion is a combination of gravitational collapse and lateral escape. In the following discussion we will use the term "lateral extrusion" merely in a non-genetic sense, implying E–W extension combined with E-directed escape. In the models of Ratschbacher (1991 a) E–W extension is in fact due to gravitational collapse. However, this may merely be a consequence of the boundary conditions chosen for the experiments, not necessarily realistic for the eastern termination of the Eastern Alps in the Pannonian basin. Note that in their experiment 1 (Ratschbacher et al. 1991 a, Fig. 4) the eastern margin of the model is practically unconfined.

Radiometric dating indicates extremely rapid uplift of the Bergell area relative to the areas to the N and S, immediately following the Bergell intrusion (Giger & Hurford 1989). Uplift was interpreted to result from vertical extrusion (Merle & Guillier 1989) by Schmid et al. (1990) which occurred during post-collisional shortening in the Late Oligocene. According to the model proposed in Fig. 4, the SW Engadine line would accommodate part of the Bergell uplift in respect to the units further to the N. Hence near the projected intersection point of Engadine line and Tonale line and within the crustal block situated within the releasing intersection of these two conjugate faults the crust reacted by vertical extrusion in response to ongoing postcollisional N–S shortening rather than by E–W extension. N of the Bergell E–W extension indicates roughly simultaneous along-strike extension, possibly related to lateral extrusion and unroofing of the Lepontine dome.

Further to the E and along strike a major change occurs regarding the response to N–S shortening. Such a change has previously been postulated in regard to movements along the Periadriatic line and associated lineaments by Schmid et al. (1989): backthrusting and related uplift of the Lepontine dome in the W versus lateral escape in the Eastern Alps further to the E. Note that Ratschbacher et al. (1991 a) successfully modelled such

a transition, but proposed lateral extrusion rather than lateral escape for the Eastern Alps. In our view the Engadine line is situated in a transitional area between the eastern margin of the Lepontine dome where vertical extrusion and uplift predominate and the Eastern Alps where lateral extrusion becomes more important. Transtension along the NE Engadine line and normal faulting within the Engadine dolomites indicate that the crustal wedge between Engadine line and Tonale line partly reacted by lateral extrusion. Very qualitatively, the analogy of this transition with the models proposed by Ratschbacher (1991 a, Fig. 4) is striking: strike-slip movements combined with folding and thrusting at the W edge of an indenter gradually change into strike-slip movements combined with an E–W stretch towards the E (lateral extrusion). In quantitative terms, however, the model 5 of Ratschbacher et al. (1991 a) probably overemphasizes the role of lateral extrusion due to somewhat problematic boundary conditions chosen for performing this experiment. The scenario in the E would result in constrictional strain at a very large scale, analogous to what was inferred for the rocks affected by minor faulting along the Engadine line on a much smaller scale. In our case the W end of the indenter would have to be searched for at the W edge of the Southern Alps (Ivrea body and Canavese line). Substantial uplift of the Bergell area at the eastern termination of the Lepontine dome rapidly decays towards the E as documented by large scale tilting of the Bergell intrusion (Reusser 1987) and the lineation pattern along the Insubric line (Schmid et al. 1989). Part of the same rotation is recorded by block rotation along the Engadine line (but note that vertical and in particular strike-slip components along the Insubric line are substantially larger). Thus, this important change in response to N–S shortening elegantly explains the block rotation inferred from Plate 1 b.

There is a problem, however, with the analogy to the work of Ratschbacher et al. (1991 a, b), both in terms of scale and timing. While these authors attempted to model the entire Eastern Alps in respect to indentation along the Giudicarie-Pustertal lines (Guidicarie indenter) and escape into the Pannonian basin, we made a direct comparison with their model in respect to the Insubric indenter further to the W. Also note that in present-day map view the Giudicarie indenter would prevent E-directed lateral extrusion as postulated for our area of investigation. We interpret the features depicted in Fig. 6 in terms of a two-stage indentation process. Indentation along the Giudicarie line (post Middle Miocene; Laubscher 1990, Martin et al. 1991, Werling 1992) is known to postdate indentation along the Canavese line (starting in the Late Oligocene, Schmid et al. 1989). As previously discussed, indentation along the Giudicarie line could possibly have led to compressional features at the front of the Oetztal nappe, overprinting the Engadine line NE of Nauders. It has to be emphasized, however, that evidence for such late NW-directed thrusting is not yet supported by detailed field work. Basically, the Oetztal nappe appears as a downfaulted block in a E–W-section between Engadine line and Brenner fault (Selverstone 1988). In analogy to the findings at the W termination of the Engadine line it is not impossible, however, to have E–W extension (Engadine line and Brenner fault) contemporaneous with NW–SE or N–S shortening (front of the Oetztal nappe).

Returning to our area of investigation the following major conclusions may be drawn:

1. There is in fact a single throughgoing Engadine line between Upper Val Bregaglia and Nauders, very probably grading into diffuse ductile deformation further to the SW

and possibly overprinted by later movements of part of the Oetztal nappe further to the NE.

2. The kinematics of movement along the Engadine line suggest oblique slip and block rotation. This complex kinematic picture is interpreted to result from a major change of the strain pattern caused by post-collisional N–S shortening occurring along strike: vertical extrusion and uplift gives way to increasing amounts of lateral extrusion towards the E. This interpretation emphasizes the need for 3-dimensional considerations, preventing simple interpretations of surface structures in terms of thickening or thinning of the entire crust.
3. Retrodeformation of the movements along the Engadine line sheds new light onto nappe correlations across this line. In particular, the Ela nappe has to be considered as Lower Austroalpine. The Silvretta-Languard-Sesvenna basement units all occupied a similar tectonic position above Lower Austroalpine or Penninic units. These basement units were first dissected by normal faulting during the Late Cretaceous and then displaced by the Late Oligocene to Early Miocene Engadine line.
4. Paleostress analysis has been shown to be useful in terms of elucidating the movement vector along brittle master faults in cases where sense-of-shear criteria are scarce or altogether missing.

Acknowledgements

This work was supported by Swiss National Science Foundation grants 21-25252.88 and 20-29869.90. Holger Stünitz is thanked for provocative remarks which led the authors to attempt a retrodeformation using nappe correlations. John Ramsay made us aware of the geometrical problems encountered when invoking block rotations. Paolo Conti is thanked for providing unpublished material on illite crystallinity. Peter Nievergelt introduced both of us into the complicated geology near Maloja. Albert Uhr is thanked for drawing Figure 1. Giorgio Dal Piaz, Guido Gosso, Roderich Mattmüller and Rudolf Trümpy improved a first version of the manuscript.

REFERENCES

ANGELIER, J. 1979: Determination of the mean principal directions of stresses for a given fault population. Tectonophysics 56, T17–T26.

ANGELIER, J. & MECHLER, P. 1977: Sur une méthode graphique de recherche des contraintes principales également utilisable en téctonique et en séismologie: la méthode des dièdres droits. Bull. Soc. géol. France (7)/XIX/6, 1309–1318.

BEARTH, P., HEIERLI, H. & ROESLI, F. 1987: Geologischer Atlas der Schweiz, 1:25000. Albulapass, Atlasblatt 81. Schweiz. Geol. Komm.

BLANCKENBURG, VON, F. 1992: Combined high-precision chronometry and geochemical tracing using accessory minerals: applied to the Central-Alpine Bergell intrusion. Chemical Geology 100, 19–40.

BUCHER-NURMINEN, K. & DROOP, G. 1983: The metamorphic evolution of garnet-cordierite-sillimanite-gneisses of the Gruf-Complex. Contr. Mineral. Petrol. 84, 215–227.

CORNELIUS, H. P. 1932: Geologische Karte der Err-Julier-Gruppe, Ost- und Westblatt, Spezialkarte 115, Schweiz. Geol. Komm.

CHEENEY, R. F. 1983: Statistical Methods in Geology. G. Allen & Unwin, London.

EBERLI, G. P. 1988: The evolution of the southern continental margin of the Jurassic Tethys ocean as recorded in the Allgäu Formation of the Austroalpine Nappes of Graubünden (Switzerland). Eclogae geol. Helv. 81, 175–214.

EUGSTER, H. 1971: Beitrag zur Tektonik des südöstlichen Graubündens (Gebiet zwischen Landwasser und Ducan). Eclogae geol. Helv. 64, 133–147.

– 1985: Beitrag zur Abklärung des Begriffes "Nordwestliche Randlinie" der Engadiner Dolomiten. Eclogae geol. Helv. 78, 215–220.

FROITZHEIM, N. 1992: Formation of recumbent folds during synorogenic crustal extension (Austroalpine nappes, Switzerland). Geology 20, 923–926.

GIGER, M. 1991: Geochronologische und petrographische Studien an Geröllen und Sedimenten der Gonfolite Lombarda Gruppe (Südschweiz und Norditalien) und ihr Vergleich mit dem alpinen Hinterland. Diss. Univ. Bern.

GIGER, M. & HURFORD, A. J. 1989: Tertiary intrusives of the Central Alps: Their Tertiary uplift, erosion, redeposition and burial in the south-alpine foreland. Eclogae geol. Helv. 82, 857–866.

GRÜNENFELDER, M. & STERN, T. W. 1960: Das Zirkon-Alter des Bergeller Massivs. Schweiz. mineral. petrogr. Mitt. 40, 253–259.

HEITZMANN, P. 1975: Zur Metamorphose und Tektonik im südöstlichen Teil der Lepontinischen Alpen. Schweiz. mineral. petrogr. Mitt. 55, 467–522.

JÄGER, E., NIGGLI, E. & WENK, E. 1967: Rb-Sr Altersbestimmungen an Glimmern der Zentralalpen. Beiträge geol. Karte Schweiz NF 134, 1–67.

KÖPPEL, V. & GRÜNENFELDER, M. 1975: Concordant U-Pb ages of monazite and xenotime from the Central Alps and the timing of high-temperature Alpine metamorphism, a preliminary report. Schweiz. mineral. petrogr. Mitt. 55, 129–132.

LAUBSCHER, H. P. 1972: Some overall aspects of Jura dynamics. Am. J. Sci. 272, 293–304.

– 1990: The problem of the deep structure of the Southern Alps: 3-D material balance considerations and regional consequences. Tectonophysics 176, 103–121.

LINIGER, M. H. 1992: Der ostalpin-penninische Grenzbereich im Gebiet der nördlichen Margna-Decke (Graubünden, Schweiz). PhD-Thesis, ETH Zürich Nr. 9769.

LINIGER, M. & GUNTLI, P. 1988: Bau und Geschichte des zentralen Teils der Margna-Decke. Schweiz. mineral. petrogr. Mitt. 68, 41–54.

MANCKTELOW, N. 1989: Stereoplot: User's Guide and Reference Manual. Unpublished manuscript.

MARTIN S., PROSSER, G. & SANTINI, L. 1991. Alpine deformation along the Periadriatic lineament in the Italian Eastern Alps. Annales Tectonicae 5, 118–140.

MATTMÜLLER, R. 1991: Überlegungen zur Deckenkinematik im Engadiner Fenster. Jb. Geol. B.-A. 134, 319–328.

MEANS, W. D. 1987: A newly recognized type of slickenside striation. J. Struct. Geol. 9, 585–590.

MERLE, O. & GUILLIER, B. 1989: The building of the Central Swiss Alps: an experimental approach. Tectonophysics 165, 41–56.

MONTRASIO, A. & TROMMSDORFF, V. 1983: Guida all' escursione del massiccio di Val Masino-Bregaglia, Val Masino occidentale, Sondrio. Mem. Soc. geol. Ital. 26, 421–434.

MOUNT, VAN, S. & SUPPE, J. 1987: State of stress near the San Andreas fault: implications for wrench tectonics. Geology 15, 1143–1146.

MÜTZENBERG, S. 1986: Ergebnisse geologischer Studien südlich Maloja. Zusammenfassung. Schweiz. mineral. petrogr. Mitt. 66, 466–472.

NIEVERGELT, P., LINIGER, M., FROITZHEIM, N. & FERREIRO MÄHLMANN, R. 1991: The Turba Mylonite Zone: An Oligocene extensional fault at the Pennine-Austroalpine boundary in Eastern Switzerland. Terra abstracts 3, 248.

OBERHAUSER, R. 1980: Das Unterengadiner Fenster. In: Der geologische Aufbau Österreichs. (Ed. by R. Oberhauser) Springer Verlag Wien, 291–299.

PFIFFNER, O. A. & BURKHARD, M. 1987: Determination of paleo-stress axes orientations from fault, twin and earthquake data. Annales Tectonicae 1, 48–57.

POZZI, R. & GIORGELLI, A. 1960: Memoria illustrativa della carta geologica della regione fra Livigno ed il passo dello Stelvio. Boll. Serv. geol. Ital. 81, 1–72.

PURDY, J. W. & JÄGER, E. 1976: K-Ar ages on rock forming minerals from the Central Alps. Mem. Ist. Geol. Mineral. Universita Padova 30, 1–31.

RATSCHBACHER, L., MERLE, O., DAVY, PH. & COBBOLD, P. 1991a: Lateral extrusion in the Eastern Alps, part 1: boundary conditions and experiments scaled for gravity. Tectonics 10, 245–256.

RATSCHBACHER, L., FRISCH, W., LINZER, G. & MERLE, O. 1991b: Lateral extrusion in the Eastern Alps, part 2: Structural analysis. Tectonics 10, 257–271.

REUSSER, E. 1987: Phasenbeziehungen im Tonalit der Bergeller Intrusion. PhD-Thesis. ETH Zürich.

SCHMID, S. M., AEBLI, H. R., HELLER, F. & ZINGG, A. 1989: The role of the Periadriatic line in the tectonic evolution of the Alps. In: Alpine Tectonics (Ed. by M. P. Coward, D. Dietrich & R. G. Park), Geol. Soc. Spec. Publ. 45, 153–171.

SCHMID, S. M. & HAAS, R. 1989: Transition from near-surface thrusting to intrabasement decollement, Schlinig thrust, Eastern Alps. Tectonics 8, 697–718.

SCHMID, S. M., RÜCK, P. & SCHREURS, G. 1990: The significance of the Schams nappes for the reconstruction of the paleotectonic and orogenic evolution of the Pennine zone along the NFP-20 East traverse (Grisons, eastern Switzerland). Mém. Soc. géol. France 156, 263–287.

SCHMUTZ, H. 1976: Der Mafit-Ultramafitkomplex zwischen Chiavenna und Val Bondasca. Beitr. geol. Karte Schweiz N. F. 149, 1–73.

SELVERSTONE, J. 1988: Evidence for east-west crustal extension in the Eastern Alps: Implications for the unroofing history of the Tauern window. Tectonics 7, 87–105.

SOMM, A. 1965: Zur Geologie der westlichen Quattervalsgruppe im schweizerischen Nationalpark. Ergebnisse der wissenschaftl. Untersuchungen im schweiz. Nationalpark 52, 1–167.

SPICHER, A. 1980: Tektonische Karte der Schweiz, 1:500000. Schweiz. Geol. Komm.

SPITZ, A. & DYHRENFURTH, G. 1914: Monographie der Engadiner Dolomiten zwischen Schuls, Scanfs und dem Stilfser Joch. Beitr. geol. Karte Schweiz N. F. 44, 1–235.

STAUB, R. 1921: Geologische Karte des Val Bregaglia. Geologische Spezialkarte der Schweiz, Blatt 90.

– 1946: Geologische Karte der Bernina-Gruppe und Umgebung. Geologische Spezialkarte der Schweiz, Blatt 118.

STÄUBLE, M. 1987: Zur Geologie zwischen dem Dreiländerpunkt, Piz Lad und Piz Ajüz. Unpublished diploma thesis, ETH Zürich.

STUTZ, E. & WALTER, U. 1983: Zur Stratigraphie und Tektonik am Nordostrand der Engadiner Dolomiten am Schlinigpass (Gemeinden Sent, Graubünden und Mals, Südtirol). Eclogae geol. Helv. 76, 525–550.

THÖNI, M. 1980: Zur Westbewegung der Oetztaler Masse. Räumliche und zeitliche Fragen an der Schlinigüberschiebung. Mitt. Ges. Geol. Bergbaustud. Österr. 26, 247–275.

– 1986: The Rb-Sr thin slab isochron method – An unreliable geochronologic method for dating geologic events in polymetamorphic terrains? Mem. Sci. geol. Univ. Padova 38, 283–352.

TRÜMPY, R. 1977: The Engadine Line: a sinistral wrench fault in the Central Alps. Mem. Geol. Soc. China 2, 1–17.

WAGNER, G., REIMER, G. M. & JÄGER, E. 1977: Cooling ages derived by apatite fission track, mica Rb-Sr and K-Ar dating: the uplift and cooling history of the Central Alps. Mem. Ist. Geol. Mineral. Universita Padova 30, 1–27.

WEBER, W. 1966: Zur Geologie zwischen Chiavenna und Mesocco. PhD-thesis ETH Zürich.

WENK, E. 1934: Der Gneiszug Pra Putér-Nauders im Unterengadin und das Verhältnis der Umbraildecke zur Silvretta-Ötztal-Decke. Eclogae geol. Helv. 27, 135–146.

WENK, H. R. 1984: Brittle-ductile transition zone in the northern Bergell Alps. Geol. Rdsch. 73, 419–431.

WERLING E. 1992: Tonale-, Pejo- und Judikarien-Linie: Kinematik, Mikrostrukturen und Metamorphose von Tektoniten aus räumlich interferierenden aber verschiedenaltrigen Verwerfungszonen. PhD-thesis ETH Zürich Nr. 9923.

ZOBACK, M. D., ZOBACK, M. L., MOUNT, VAN, S., SUPPE, J., EATON, J. P., HEALY, J. H., OPPENHEIMER, D., REASENBERG, P., JONES L., RELEIGH, C. B., WONG, I. G., SCOTTI, O. & WENTWORTH, C. 1987: New evidence on the state of stress of the San Andreas fault system. Science 238, 1105–1111.

Manuscript received 17 June 1992
Revised version accepted 12 January 1993

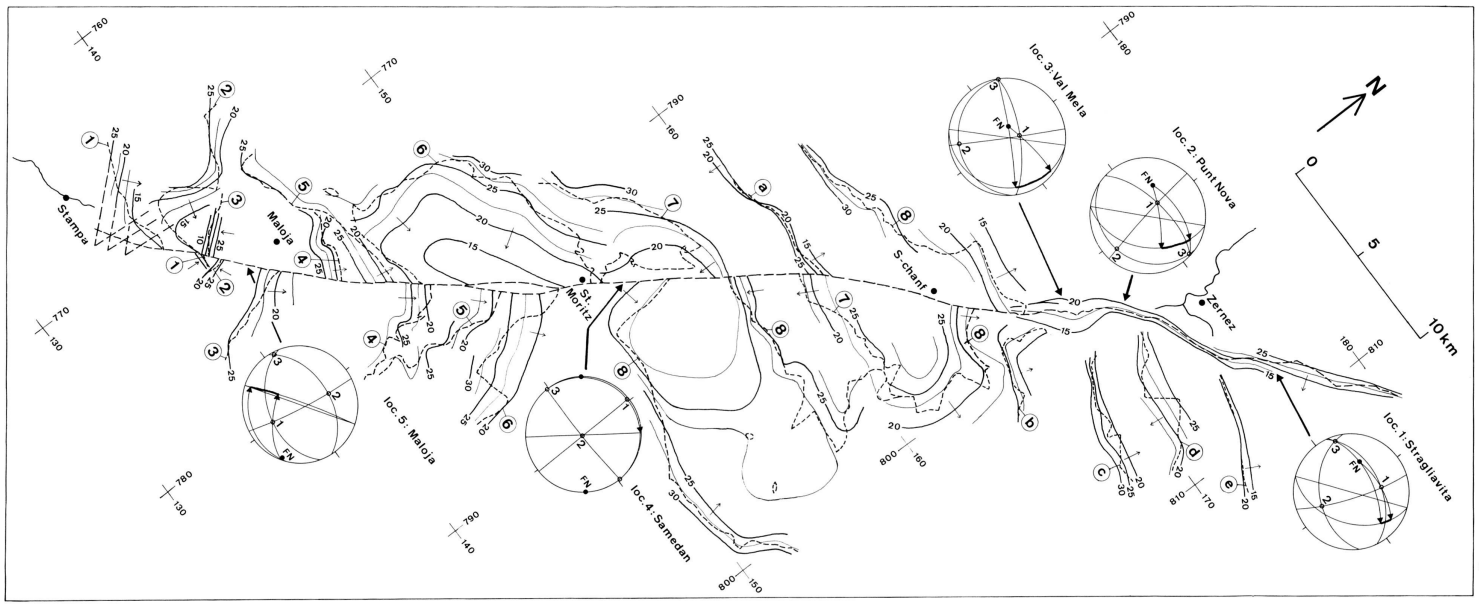
Stampa
Maloja
St. Moritz
S-chanf
Zernez
loc. 1: Stragliavita
loc. 2: Punt Nova
loc. 3: Val Mela
loc. 4: Samedan
loc. 5: Maloja
N
0
5
10 km

a

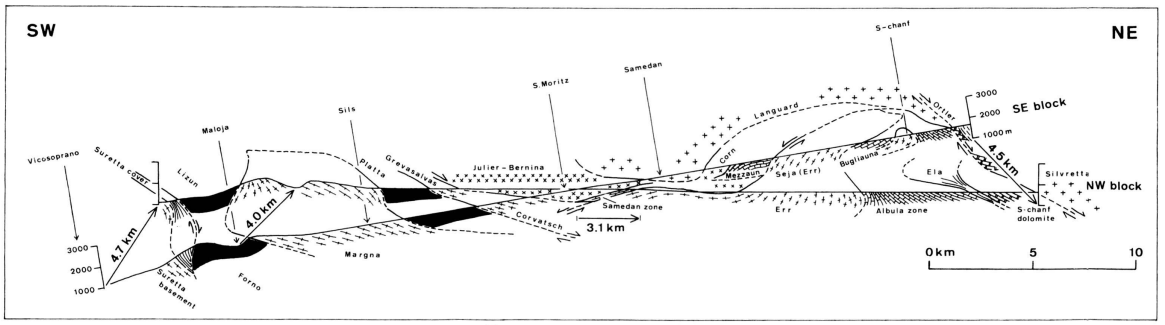
SW
NE
Vicosoprano
Surretta cover
Lizun
Maloja
Sils
Piatta
Grevasalvas
Julier – Bernina
S.Moritz
Samedan
S-chanf
Languard
Corn
Margun
Seja (Err)
Bugliaun
Ela
Silvretta
NW block
SE block
3000
2000
1000 m
4.5 km
4.7 km
4.0 km
3.1 km
Surretta basement
Forno
Margna
Corvatsch
Samedan zone
Err
Albula zone
S-chanf dolomite
0 km
5
10

b

Plate 1.

a. Contour map of major tectonic surfaces (contour interval 250 m) including location of the 5 localities used for paleostress determination along the Engadine line. Stereograms indicate the best fit orientation of the principal axes of stress labelled 1, 2, 3 (for σ_1, σ_2 and σ_3 respectively), the orientation of the Engadine line master fault (FN is the fault plane normal), the corresponding great circle and the range of possible movement directions within the plane of the master fault (arrows joining the great circle representing the master fault).

Apart from the Engadine line (only contoured NE of S-chanf) the following tectonic surfaces have been contoured: 1, top Suretta basement; 2, Turba mylonite zone; 3, base Margna nappe; 4, top Margna nappe; 5, base Grevasalvas and Corvatsch unit (Err nappe); 6, base Julier-Bernina nappe; 7, top Err basement s.str. and top Seja basement (Err basement s.l., identical with the Mezzaun normal fault, compare Fig. 5b); 8, base of the Upper Austroalpine nappes (Languard nappe, Ortler zone and Silvretta nappe); a, front of the Err nappe s.str.; b–e, normal faults within the Engadine dolomites (b, at the base of the Quattervals unit; c, d, at or near the base of the Terza unit; e, Chavagl fault).

b. Two vertical profiles parallel to the trace of the Engadine line, constructed on the basis of the contours given in (a). While the profile concerning the NW block is held fixed, the profile concerning the SE block has been retrodeformed in order to obtain an optimal fit in regard to the tectonic boundaries labelled 1–6 in (a). The vectors indicate the translation within the fault plane needed in order to obtain the present day configuration. Arrows indicate sense of movement along normal faults of presumably Late Cretaceous age.